Polymer Chemistry

ROYAL SOCIETY OF CHEMISTRY

PAPER

View Article Online
View Journal | View Issue

Cite this: *Polym. Chem.*, 2024, **15**, 2240

A proof-of-concept study on a fully biobased and degradable polymer network based on vanillin and myrcene†

Pia S. Löser,[a] Arthur Lamouroux,[b] Michael A. R. Meier[a,c] and Audrey Llevot *[b]

Received 8th March 2024,
Accepted 9th May 2024

DOI: 10.1039/d4py00269e

rsc.li/polymers

Despite the widespread use of polymer networks, their development has tended to disregard crucial sustainability considerations. In particular, their production and their management at the end-of-life can generate high environmental impacts. Therefore, the design of fully biobased and degradable polymer networks is of great importance. In this work, vanillin and myrcene were selected as renewable resources and a carbonate unit as cleavable linkage to induce a possible network disassembly. Vanillin was converted into a symmetric α,ω-diene featuring a carbonate unit in its center. This monomer was copolymerized by thiol–ene reaction with a myrcene derived trithiol to form a polymer network. An elastic transparent film exhibiting a glass transition temperature of 14 °C, a Young's modulus of 6.87 MPa, an ultimate tensile strength of 1.48 MPa and an elongation at break of 148% was obtained. Owing to the inherent carbonate group, the polymer network could be degraded under acidic conditions into a polyol with an OH content of 2.23 mmol g^{-1}, as determined by ^{13}P NMR. The polyol obtained by degradation was effectively repolymerized to produce a new polyurethane. These proof-of-concept findings provide a potential strategy for circularization of biobased polymer networks.

Introduction

Reducing the environmental impact of cross-linked polymers is a crucial matter for our society. Over the last decades, this topic has become the focus of many researchers, both in academia and industry, as cross-linked polymers are extensively employed. Initial efforts were mainly devoted to the transition from fossil to renewable feedstocks. Terpenes, vegetable oils, lignin, carbohydrates and thereof derived platform chemicals have been used successfully for the synthesis of polymer networks, including epoxy, polyurethane and polyester resins.[1–5] These first steps towards more sustainable polymer networks are important, but problems arising at their end-of-life should also be addressed. The permanently cross-linked nature of these materials provides them with outstanding thermo-mechanical properties and chemical resistance. These characteristics are the driving factors behind their applications in the field of automotive, aerospace, electronics, construction *etc*. However, this structure hinders their recyclability, traditionally limiting their end-of-life options to either incineration or grinding for filler applications.[6] To tackle this issue, the introduction of degradable and/or dynamic units as cross-links or into the polymer backbone has been proposed. Different concepts, such as covalent adaptable networks, vitrimers, structurally tailored and engineered macromolecular networks, living additive manufacturing or macromolecular metamorphosis have emerged to ensure the post-modification or recycling of polymer networks.[7–12] In order to decrease the environmental impact of polymer networks, combining recyclability with the use of bioresources is crucial.[13–19]

Among all the biobased monomers used for the preparation of polymer networks, vanillin is an interesting precursor due to its aromatic structure and its aldehyde and phenolic functional groups. Vanillin, which is historically extracted from vanilla beans, can also be industrially produced from lignosulfonates, a side-product of the sulfite pulping industry. A large number of studies report the synthesis of polymer networks from vanillin, which are also summarized in a few reviews.[20–24] Contrary, the literature about biobased recyclable vanillin-based polymer networks is less abundant. This field is dominated by the preparation of vitrimers featuring dynamic imine

[a]*Laboratory of Applied Chemistry, Institute of Organic Chemistry (IOC), Karlsruhe Institute of Technology (KIT), Straße am Forum 7, 76131 Karlsruhe, Germany*
[b]*Univ. Bordeaux, CNRS, Bordeaux INP, LCPO, UMR 5629, F-33600 Pessac, France. E-mail: audrey.llevot@enscbp.fr*
[c]*Laboratory of Applied Chemistry, Institute of Biological and Chemical Systems – Functional Molecular Systems (IBCS-FMS), Karlsruhe Institute of Technology (KIT), Hermann-von-Helmholtz-Platz 1, 76344 Eggenstein-Leopoldshafen, Germany*

†Electronic supplementary information (ESI) available: Characterization data: ^{1}H NMR and ^{13}C NMR spectra, DSC analyses and FTIR spectrum of the polyurethane. See DOI: https://doi.org/10.1039/d4py00269e

motives.[25–32] Moreover, different synthetic approaches have been described to synthesize polyimine networks,[33–35] imine/epoxy networks,[36–39] imine/urethane networks[40–42] or polymer networks by radical polymerization.[43] Dihydrazone-based dynamic covalent epoxy networks,[44] vinylogous urethane vitrimers[45] and disulfide-based epoxy vitrimers[46] were also produced.

Alternatively, in line with the Green Chemistry concept "design to degrade", the presence of cleavable units enables the degradation of polymer networks into monomers or oligomers that can potentially be repolymerized or used as value-added chemicals for other applications.[47] In 1996, Buchwalter and coworkers reported the design of cycloaliphatic diepoxides featuring a cleavable linkage (ketal, acetal, formal or ester) for the preparation of thermosets capable of being disassembled in acid-containing solvent mixtures.[48] Vanillin constitutes a relevant building block to apply this strategy to biobased polymer networks. For instance, the ester moiety introduced during the synthesis of doubly glycidylated vanillic acid (at the hydroxyl and the carboxylic acid group), in combination with the presence of ester moieties in epoxidized soybean oil, was used as disassembly points for the degradation of fully biobased epoxy resins in acidic media.[49,50] Vanillin was also converted into an α,ω-diene monomer with degradable ester groups in its center *via* Williamson and Tishchenko reactions and reacted with multifunctional thiols to form degradable thermosets.[51] Vanillin-based degradable epoxy resins were synthesized using monomers incorporating Schiff base linkages.[52,53] Several monomers exhibiting acetal groups in their center were also prepared from vanillin by exploiting its aldehyde group. Wu and coworkers synthesized an α,ω-diene monomer by Williamson reaction followed by acetalization in the presence of pentaerythritol.[54] This monomer was converted to a degradable polymer network by thiol–ene reaction, with potential applications in flexible devices. A spirodiacetal building block was synthesized by Lin and coworkers by reacting vanillin with erythritol.[55] This cleavable monomer was copolymerized with epoxidized soybean oil to yield a fully biobased polymer network. Owing to the dynamic and degradable features of acetal motive, the obtained materials exhibited both good recyclability (covalent adaptable network) and acid degradability, and the degraded products could be reused for the preparation of new polymer networks.

Carbonates represent an interesting class of dynamic and acid-degradable linkages that have not been deeply investigated for the preparation of recyclable polymer networks up to date. In 2000, Wong and coworkers synthesized cycloaliphatic epoxides containing thermally cleavable carbonate linkages. These monomers underwent curing reactions with cyclic anhydrides, similarly to a commercial cycloaliphatic diepoxide and the resulting polymer networks could be disassembled at 220 °C.[56] Recently, transcarbonation reactions in the presence of free hydroxyl groups were exploited to prepare acid-degradable polycarbonate vitrimers.[57] To the best of our knowledge,

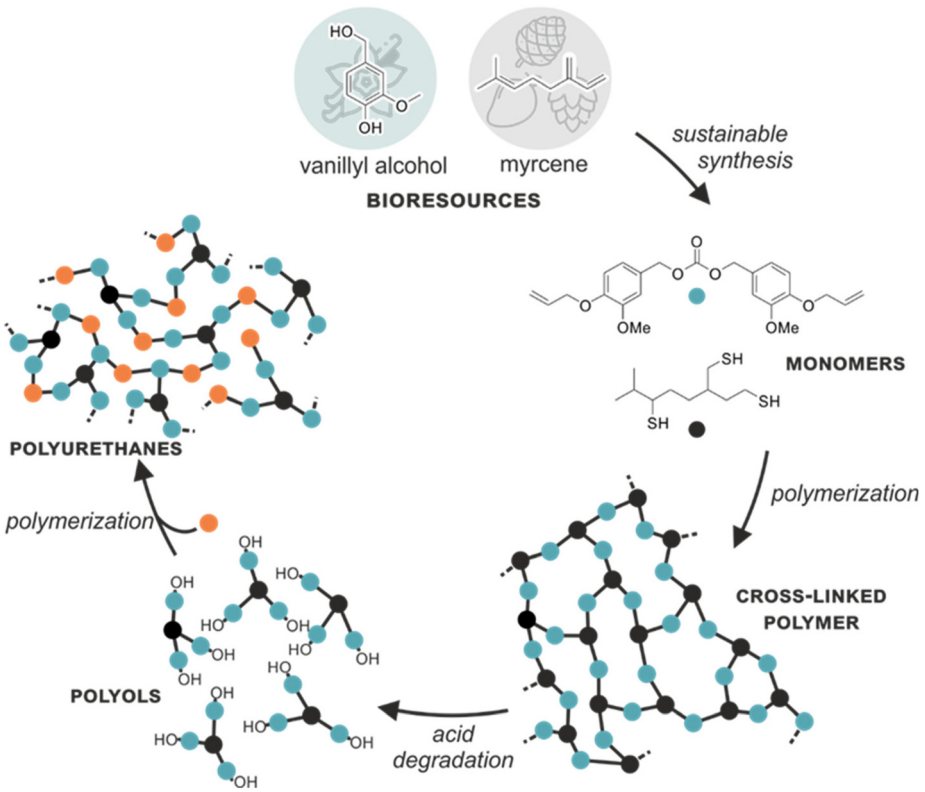

Fig. 1 General strategy implemented in this study.

there is no example of degradable and fully biobased polymer network based on cleavable carbonate units.

In this work, a symmetric α,ω-diene monomer featuring a cleavable carbonate unit in its center was designed from vanillyl alcohol. A myrcene-based trithiol was further synthesized as biobased comonomer for thiol–ene polymerization. The photopolymerization of these monomers and the thermomechanical properties of the obtained polymer network were studied. Subsequently, the cleavage of the symmetric monomer was investigated as a model, before transferring the most promising conditions to the polymer networks. Finally, the polyols obtained as degradation products were thoroughly characterized and repolymerized into polyurethanes to demonstrate the feasibility of reusing the degraded polymer network (Fig. 1).

Results and discussion

A cleavable α,ω-diene (**AVACarb**) was synthesized from vanillyl alcohol in a 2-step approach. The difference of reactivity between the phenolic and benzylic hydroxyl groups of vanillyl alcohol was exploited to selectively introduce the two desired functionalities: first allyl groups for later thiol–ene polymerization and subsequently a cleavable carbonate linker (Scheme 1).

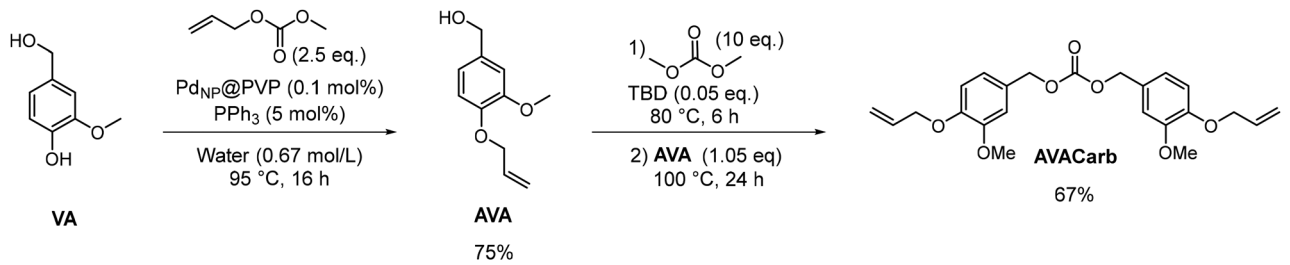

Scheme 1 Reaction scheme of the synthesis of the cleavable α,ω-diene: allylated vanillyl alcohol carbonate (**AVACarb**).

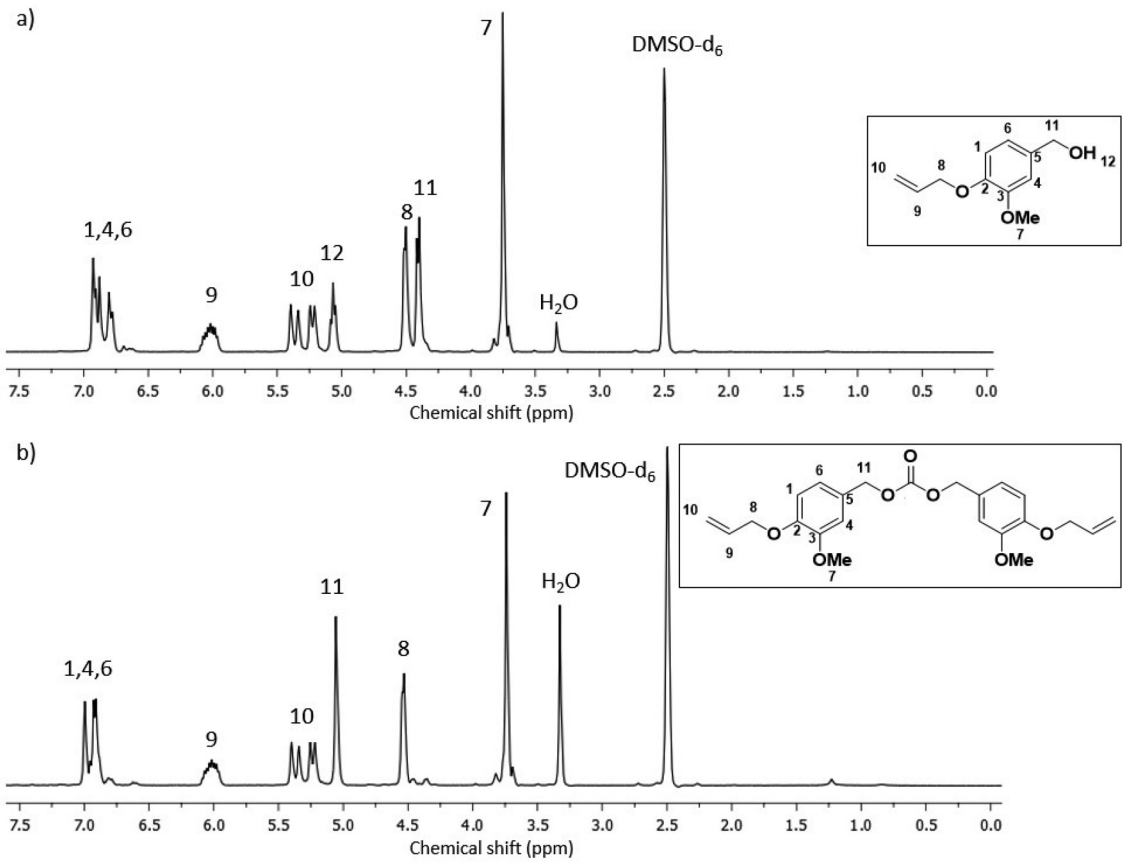

Fig. 2 ^{1}H-NMR spectra of allylated vanillyl alcohol **AVA** (a) and the cleavable α,ω-diene **AVACarb** (b) in DMSO-d$_6$.

The allylation of vanillyl alcohol (**VA**) was carried out *via* Tsuji–Trost reaction in water employing palladium nanoparticles stabilized on poly(vinyl pyrrolidone) (PVP) as catalyst, triphenyl phosphine as additive and allyl methyl carbonate as allylating agent.[58] This procedure enabled a selective allylation of the phenolic hydroxyl group, as evidenced by the unmodified peak of the benzylic OH group in the ^{1}H NMR spectrum at 5.08 ppm (signal 12 Fig. 2a). After extraction, **AVA** was obtained in a yield of 75%. This methodology constitutes a sustainable alternative to classic allylation reactions using reactants such as allyl halides. A symmetric cleavable α,ω-diene (**AVACarb**) was then synthesized from **AVA** using potentially renewable and non-toxic dimethyl carbonate (DMC) and 1,5,7-triazabicyclo [4.4.0]dec-5-ene (TBD) as organocatalyst.[59] The carbonate moiety was introduced in a 2-step procedure. **AVA** was reacted with 10.0 eq. of DMC and 5.00 mol% TBD at 80 °C. After 6 h reaction time, **AVA** was almost completely converted into vanillyl methyl carbonate. Subsequently, the excess of DMC was removed under reduced pressure and 1.05 eq. **AVA** were added. The mixture was heated to 100 °C for 24 h without additional solvent, as the higher temperature enabled the reaction to proceed in a molten state. After purification, the symmetric allylated vanillyl alcohol carbonate (**AVACarb**) was obtained in a 67% yield. The structure of this monomer was confirmed by ^{1}H NMR (Fig. 2b). The disappearance of the peak at 5.08 ppm (signal 12), characteristic of the proton of the benzylic OH group and the shift of the peak characteristic of the benzylic CH_2 from 4.43 ppm to 5.06 ppm (signal 11) due to the incorporation of the adjacent electron-withdrawing carbonate group were observed. This monomer was also characterized by ^{13}C NMR, mass spectrometry and IR spectroscopy (see ESI†).

A biobased trithiol was synthesized from myrcene, following a 2-step procedure described before for the preparation of limonene dithiol (Scheme 2).[60]

In a first step, myrcene was reacted with thioacetic acid by stirring the mixture at room temperature for 23 h. The reaction was monitored by gas chromatography (GC) (Fig. 3a). The disappearance of the signal at 2.4 min, attributed to myrcene, and the appearance of a new signals at 16 min indicated the completion of the reaction. Subsequently, unreacted thioacetic acid was removed under reduced pressure. Then, a transesterification was performed in methanol in the presence of TBD as catalyst. The solution was stirred at 75 °C for 25 h to cleave the thioester groups. The GC chromatogram (crude product) showed the disappearance of the signals at 16 min and the appearance of three main signals at 9.8, 10.5 and 11.2 min. The separation of the products was attempted by column chromatography. The 1st collected fraction mostly contained by-products. Fractions 2 and 3 both contained a mixture of the main products, which consist of stereo- and regio-isomeric

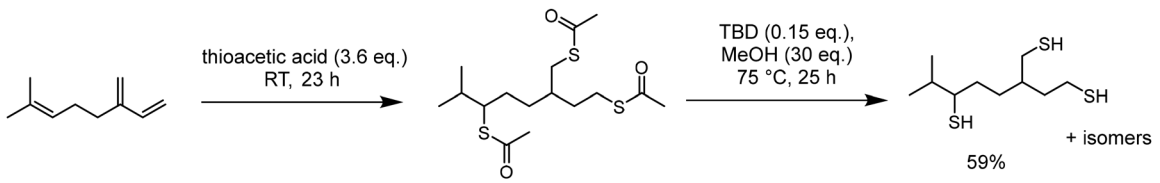

Scheme 2 Reaction scheme of the synthesis of myrcene trithiol monomer.

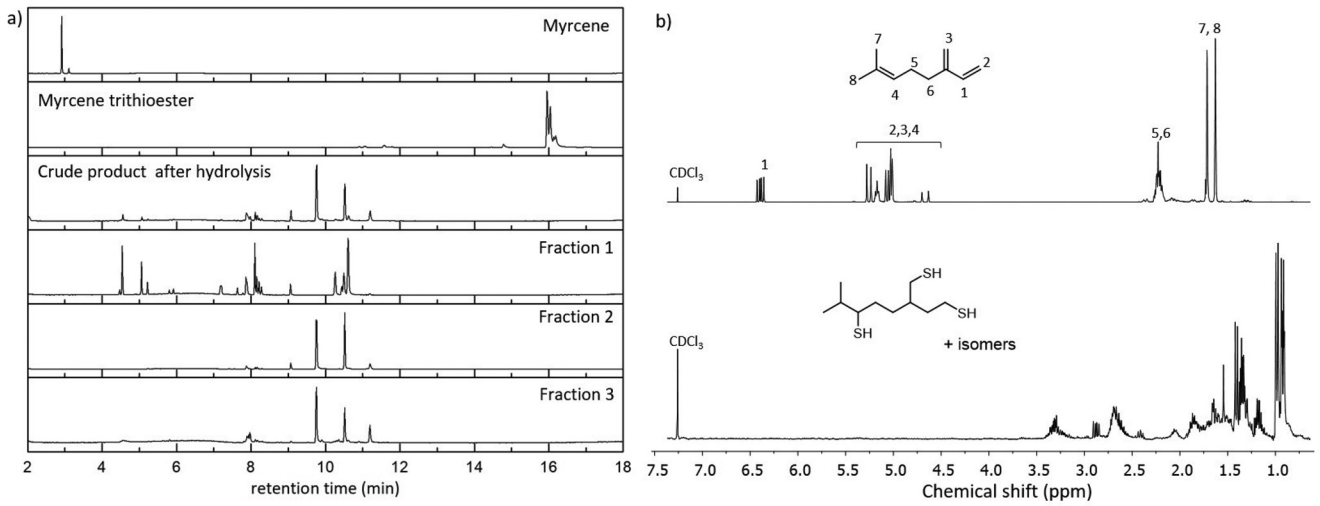

Fig. 3 (a) GC-MS monitoring of the synthesis of myrcene trithiol, from the top to bottom: starting material myrcene, reaction mixture after reaction with thioacetic acid for 23 h, crude product after thioester hydrolysis, fraction 1, fraction 2 and fraction 3 collected after column chromatography, (b) ^{1}H NMR spectra of myrcene (top) and fraction 2 (bottom) in $CDCl_3$.

structures, explaining the multiple peaks observed by GC analysis. These two fractions, which represented a yield of 58%, were gathered and further analyzed. Compared to myrcene, the ^{1}H NMR of the product confirmed the complete conversion of the double bonds (Fig. 3b). The appearance of peaks between 2.5 and 3.5 ppm, characteristics of protons adjacent to the thiol moiety is observed. The ^{13}C NMR showed a multitude of peaks which were attributed to CH, CH_2 and CH_3 with the help of DEPT and HSQC analyses (Fig. S4 and S5†). However, due to the presence of several isomers (potentially regio and stereo isomers), peaks could not be assigned precisely. Therefore, the structure of the trithiol was assessed by elemental analysis ($C_{10}H_{22}S_3$, calculated: C 50.37%, H 9.30%, S 40.33%; found: C 50.67%, H 8.61%, S 38.67%) and mass spectrometry (EI-HRMS of $C_{10}H_{22}S_3$ $[M]^+$, calculated: 238.0878; found: 238.0882). In the literature, the synthesis of this trithiol has been reported in a patent.[61] In this case, thiol formation was achieved by radical and acid-catalyzed sulfhydration of

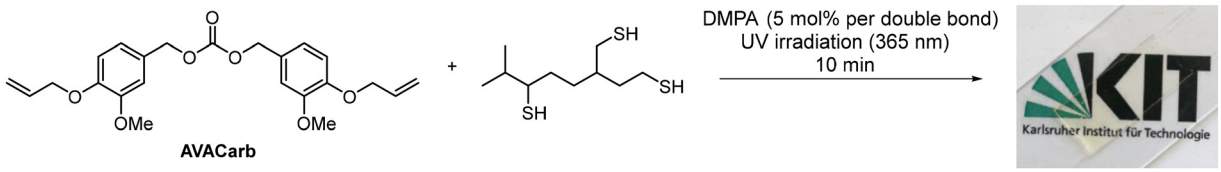

Fig. 4 Thiol–ene coupling between **AVACarb** and myrcene-based trithiol resulting in a cross-linked polymer film (picture).

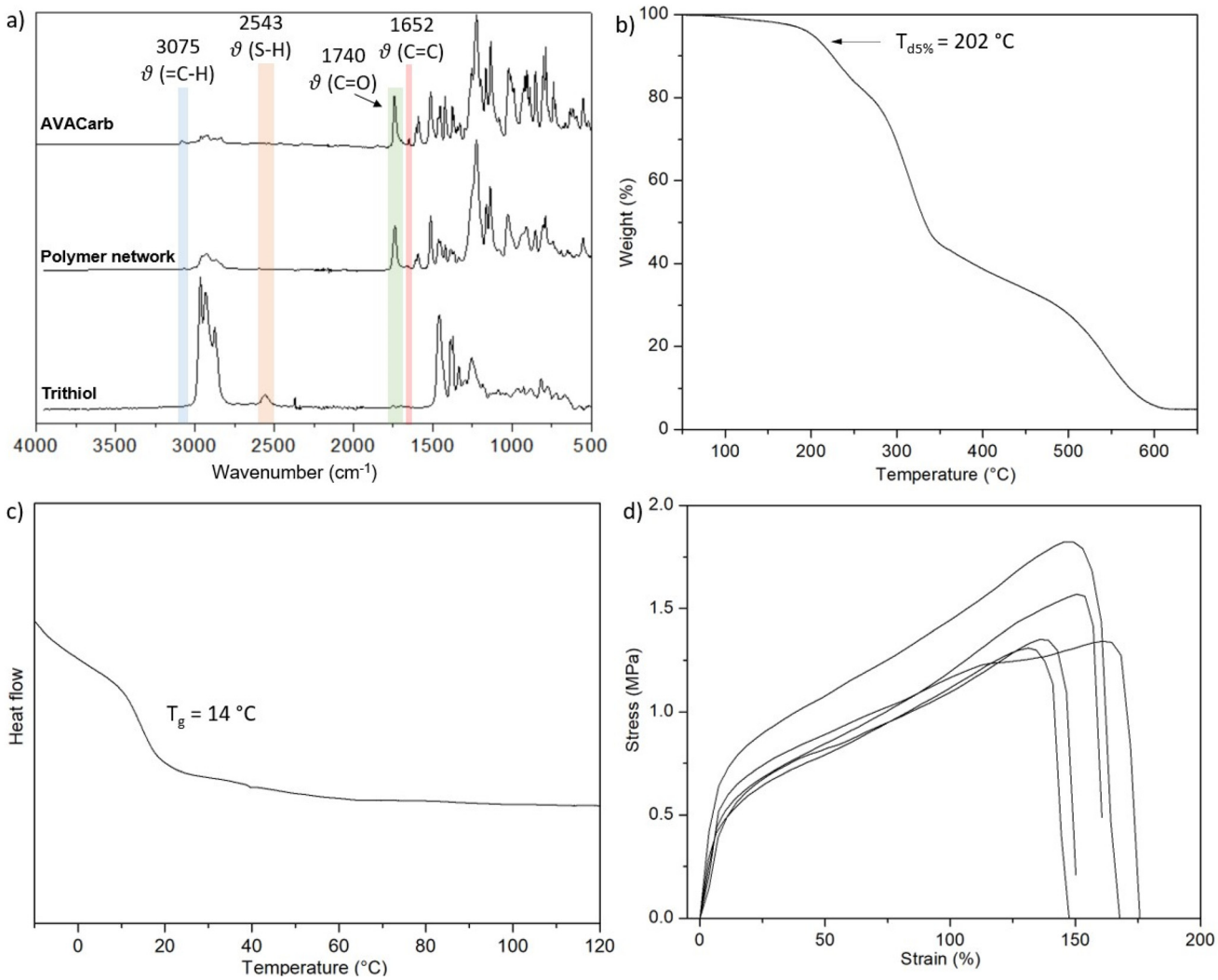

Fig. 5 (a) FTIR spectra of myrcene trithiol (bottom), **AVACarb** (top) and resulting film (middle); (b) TGA thermogram, (c) DSC thermogram, (d) tensile tests (5 replicates), of polymer films obtained by thiol–ene polymerization of myrcene trithiol and **AVACarb**.

myrcene using H_2S as sulfur source. After distillation, the product was also obtained as a mixture of regioisomers in a purity of 98%, but no characterization was provided.

Having both monomers in hand, thiol–ene polymerization was investigated (Fig. 4). The monomers were mixed in a double bond : thiol ratio of 1 : 1 in the presence of 2,2-dimethoxy-2-phenylacetophenone (DMPA) as initiator. In order to prepare films, the mixture was gently heated to ensure melting of the monomers and was poured onto a glass plate. The samples were placed in a UV-oven and irradiated at 365 nm for 10 min. After polymerization, the resulting transparent free-standing film could be peeled off the glass plate. FTIR was used to verify the completion of the thiol–ene photopolymerization (Fig. 5a).[62] Full conversion of the thiol was observed through disappearance of the peak located at 2543 cm^{-1} (S–H stretching). The signals associated to the allyl groups at 1647 cm^{-1} (C=C stretching), and 3075 cm^{-1} (olefinic =C–H stretching) showed very low intensity and a significant decrease compared to the **AVACarb**. FTIR analyses of the polymer film also highlighted the presence of C=O vibration at 1738 cm^{-1}, indicating that the carbonate remained unaffected during the cross-linking reaction (Fig. 5a). Moreover, this fact was confirmed by the synthesis and characterization of a model thiol–ene adduct from **AVACarb** and 2 equivalents of 2-phenylethanethiol (see ESI pp. 4–9†). The polymer film exhibited a relatively low soluble fraction in THF (14 wt% soluble fraction), a glass transition temperature (T_g) of 14 °C and a temperature at 5% weight loss ($T_{d5\%}$) of 202 °C (Fig. 5b and c).

Tensile test measurements were performed on 5 replicates to determine the mechanical properties and show the reproducibility of the synthesis. The film exhibited a Young's modulus of 6.87 ± 1.29 MPa, an ultimate tensile strength of 1.48 ± 0.194 MPa and an elongation at break of 148 ± 10.7% (Fig. 5d). These mechanical properties fall in the same range as similar systems based on vanillin or lignin derivatives thiol–ene networks.[51,54,62,63] Finally, the crosslinking density (ν_e) was calculated from the classical rubbery elasticity theory by DMA analysis (Fig. S12†). A value of 50 mmol dm^{-3} lying in the low range of what has been reported in the literature for similar systems, *i.e.* polymer networks synthesized by thiol–ene reaction, was obtained.[54,64] The polymer film obtained in this study constituted a good base to investigate the degradability of the carbonate linker in a polymer network. A deeper screening of the polymerization conditions could lead to a decrease of the soluble fraction and an increase of the cross-linking density and thus, polymer thermomechanical properties.

With the objective to develop a solvent-assisted depolymerization method for the polymer networks, the cleavage conditions of the carbonate units were first screened using the **AVACarb** monomer (Fig. 6a). The cleavage of **AVACarb** into **AVA** was monitored by size exclusion chromatography (SEC). We normalized the peak characteristic of **AVACarb** (retention time: 34 min) and observed the appearance and further increase of a peak at 36 min characteristic to **AVA** (Fig. 6b). The structure of the obtained **AVA** was also confirmed by GC-MS (Fig. S14†). The integration of these peaks enabled the estimation of a degradation percentage when screening different reaction con-

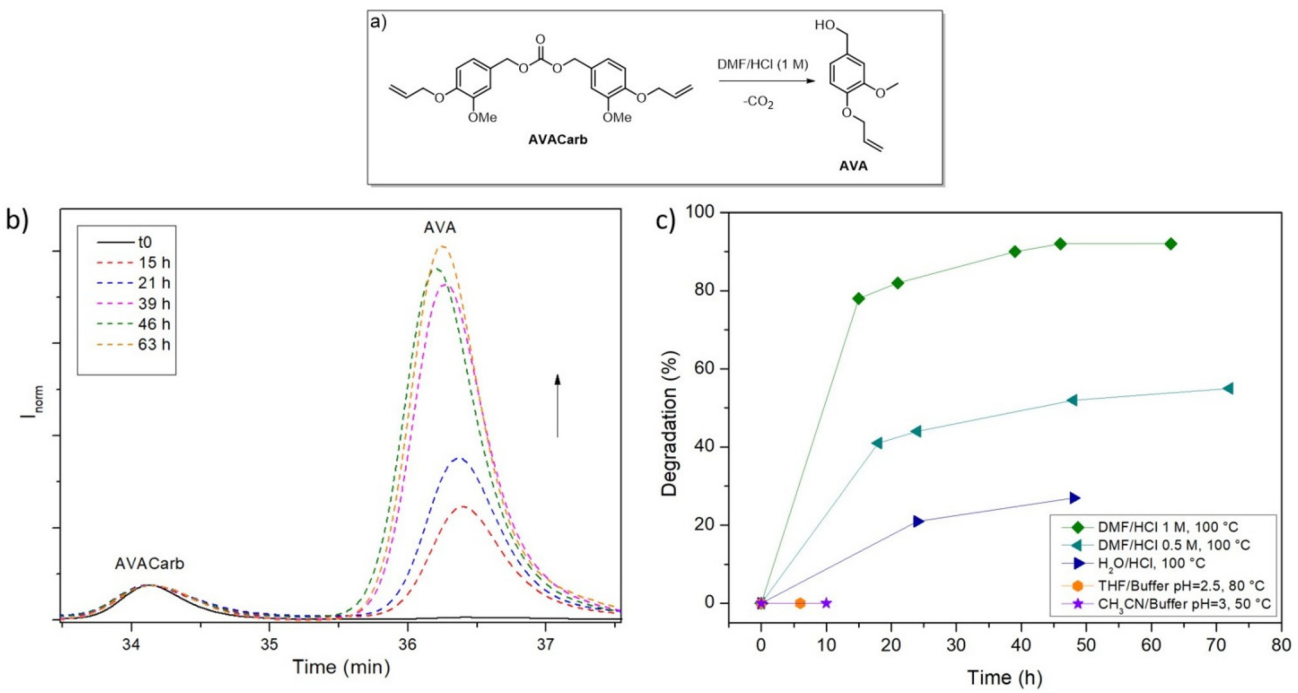

Fig. 6 (a) Molecular model: cleavage of **AVACarb** into **AVA** under acidic conditions, (b) monitoring of the degradation in DMF/HCl 1 M at 100 °C *via* SEC, (c) establishment of degradation conditions for **AVACarb**: test of different reaction conditions.

ditions for the degradation (Fig. 6c). The use of DMF as organic solvent proved to be beneficial to solubilize both the starting material and degradation product. The increase of the acid concentration (from 0.5 M to 1 M) led to a faster and more complete degradation. Under optimized conditions, 92% of the **AVACarb** was degraded into **AVA** within 46 h.

Following the promising degradation results of **AVACarb**, the suitability of the established procedure was evaluated on the polymer network. Initially, the sample was insoluble in the DMF/HCl mixture. After 24 h however, complete solubilization was observed (Fig. 7a) and the degradation of the solubilized polymer could be monitored by SEC (Fig. 6b). From 24 h to 73 h, the SEC trace of the degradation product showed a shift to lower molar masses and a decrease of the dispersity. The reaction time was prolonged to 120 h, but no further polymer network disassembly could be observed. The solvent was removed under reduced pressure and the resulting powder was analyzed by ESI-MS. The most abundant peak (855.3418 g mol^{-1}) could be assigned to the expected degradation product (Fig. 6c and d), consisting of the myrcene trithiol linked to three **AVA** moieties. The good agreement between the measured and the calculated isotopic patterns (Fig. 7e) of this product confirmed its structure. This structure identification confirms that (i) the network can be degraded as expected and moreover that (ii) the cross-links within the network were formed as anticipated.

Further characterization was performed to confirm the chemical structure of the degradation product. The hydrolysis of the carbonate group was confirmed by FTIR with the disappearance of the band at 1738 cm^{-1} (Fig. 8a) and by ^{13}C NMR with the absence of peak between 155 and 157 ppm (Fig. 8b). In both analyses, a new signal characteristic of another carbonyl function at 1718 cm^{-1} in the FTIR spectrum and at 161 ppm on the ^{13}C NMR spectrum was detected. We suggest that these signals belong to a carbonic acid monobenzylester, which is an intermediate in the hydrolysis reaction

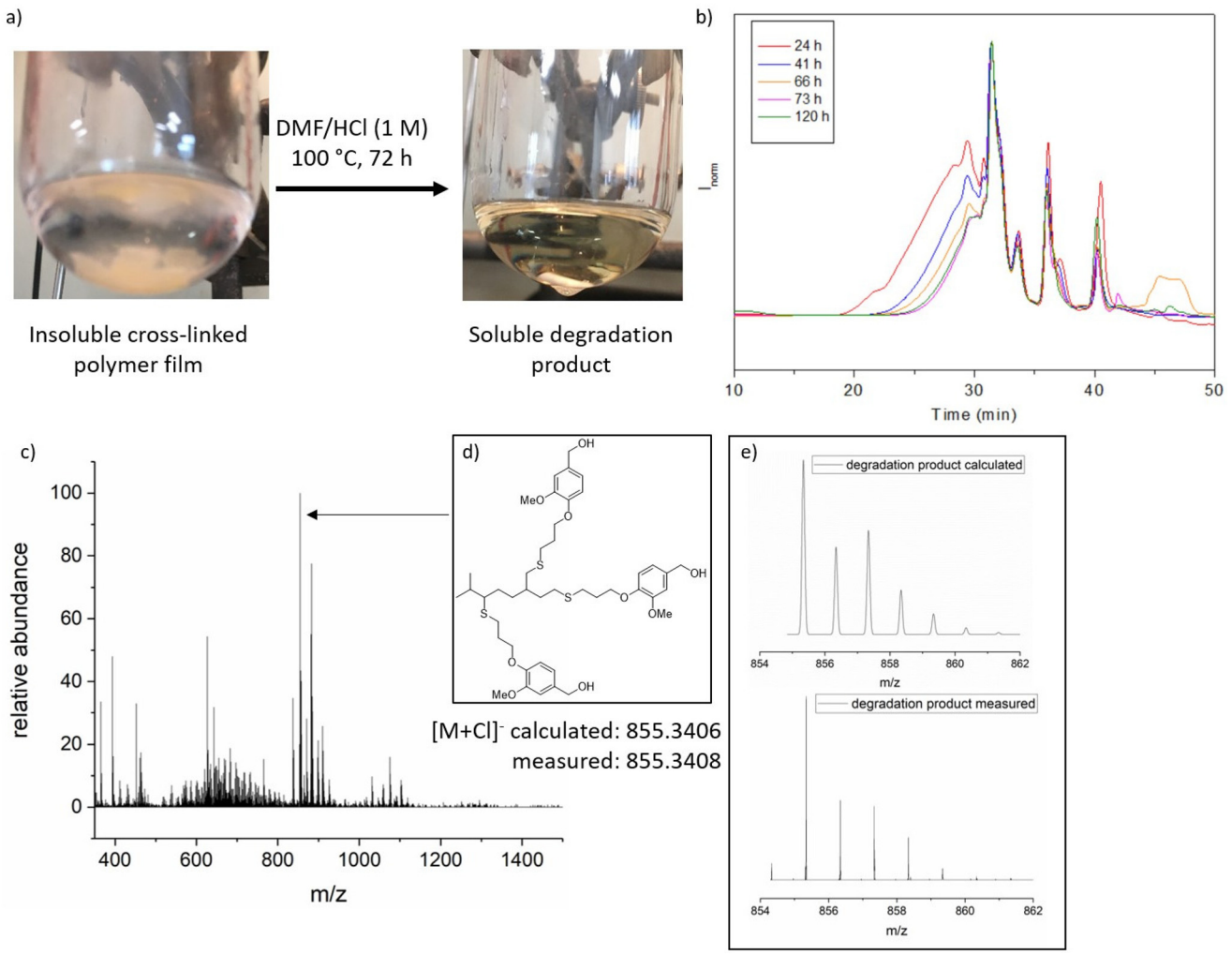

Fig. 7 (a) Visual observation of the cross-linked polymer solubilization under degradation conditions, (b) SEC monitoring of the solubilized polymer, (c) ESI-MS spectrum of degradation product, (d) chemical structure of the expected main degradation product, (e) calculated isotopic pattern (top), measured isotopic pattern of the expected degradation product.

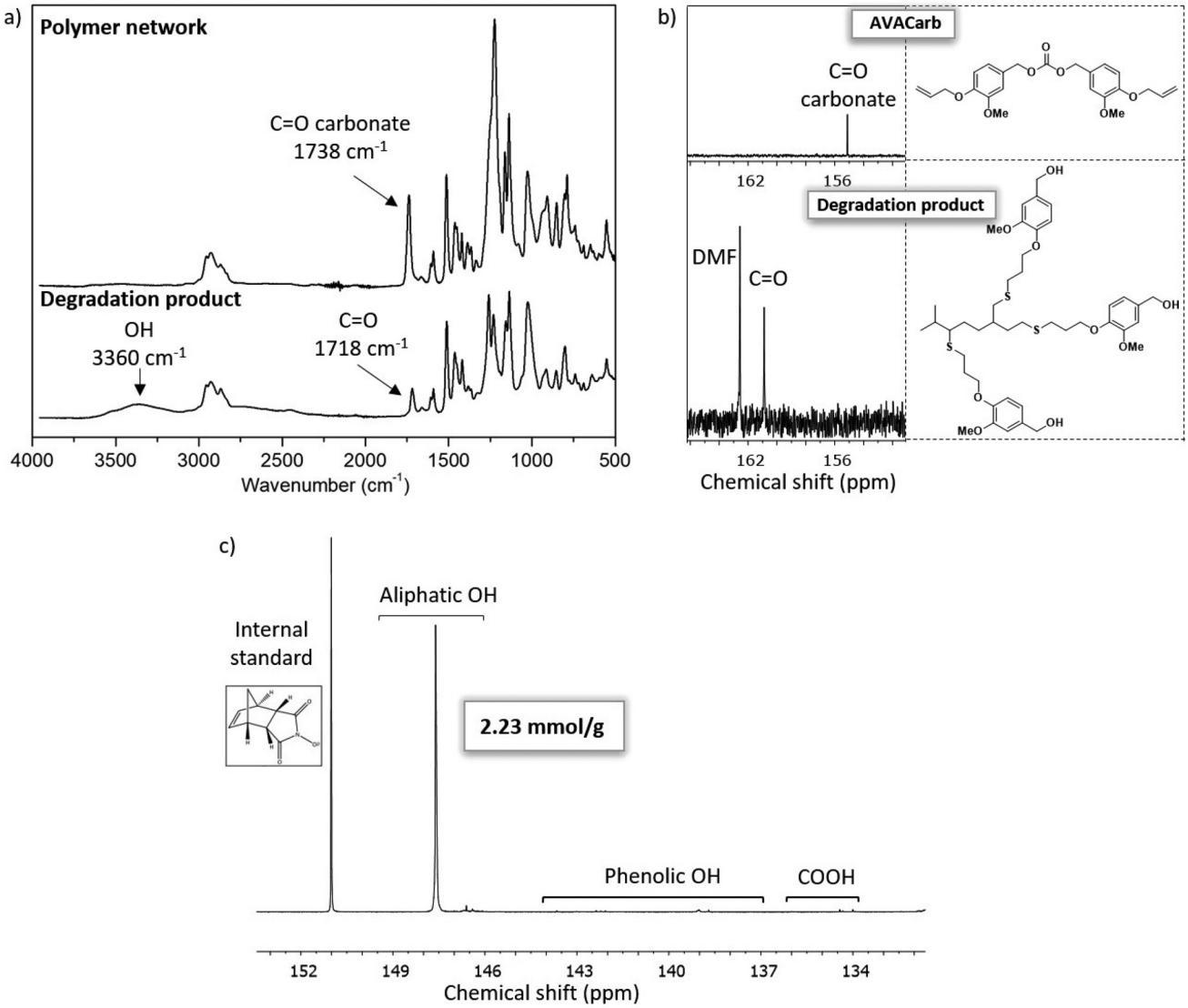

Fig. 8 (a) FTIR spectra of the polymer network (top) and degradation product (bottom), (b) zoom on the ^{13}C NMR spectra of the **AVACarb** (top) and degradation product (bottom), (c) ^{31}P NMR spectrum of the phosphorylated degradation product.

(Scheme S2†). Monoesters of carbonic acid are known to be unstable and tend to decompose into alcohol and carbon dioxide, but some studies reported their isolations, especially in acidic solutions.[65–68] Additionally, the FTIR spectrum of the degradation products revealed the appearance of a band attributed to OH vibrations at 3360 cm^{-1}. The identification of the nature of hydroxyl groups and their quantitative determination has been carried out by ^{31}P NMR spectroscopy. For this analysis, the degradation product was phosphorylated using 2-chloro-4,4,5,5-tetramthyl-1,3,2-diaxophospholane and the proportions of each type of hydroxyl group were evaluated against an internal standard (*N*-hydroxy-5-norbornene-2,3-dicarboximide).[69] The ^{31}P NMR spectrum of the degradation product exhibited one main peak at around 147 ppm, the area of aliphatic hydroxyl groups (Fig. 8c). By relative integration to the internal standard, an OH content of 2.23 mmol g^{-1}, corresponding to 124 mg KOH per g, was calculated for the polyol received by network degradation. This value is in the range of commercially available polyols prepared from vegetable oils constituting classic building blocks for polyurethane synthesis (Table S1†).[70]

As a preliminary test of the degradation product's reactivity in polyurethane synthesis, the obtained polyol was mixed with 4,4′-methylene-bis(cyclohexyl isocyanate) (HMDI) in a DSC pan in the presence of dibutyltin dilaurate catalyst. During the first heating ramp, an exothermic peak characteristic of the polymerization was observed (Fig. S15†). Afterwards, the resulting polymer exhibited a T_g of 9 °C (Fig. S16†). The success of the repolymerization was also confirmed by FTIR with the disappearance of the isocyanate stretching vibration at 2246 cm^{-1}, the decrease of the alcohol stretching vibration at 3360 cm^{-1} and the appearance of the stretching vibration of

the urethane C=O bond at 1710 cm^{-1} and of the bending vibration of the N–H bond at 1560 cm^{-1} (Fig. S17†). Acknowledging the extensive range of applications of polyurethanes, the valorization of degradation products for their synthesis is a promising approach for the chemical recycling of materials and especially cross-linked polymers.

Conclusions

A vanillin-derived α,ω-diene monomer featuring a carbonate linkage in its center was synthesized and copolymerized with a biobased myrcene-based trithiol. The obtained fully biobased polymer network exhibited a relatively low soluble fraction, elastic properties and good thermal properties. The presence of the cleavable carbonate unit endows the polymer network with good degradation properties. In a DMF/HCl mixture at 100 °C, the polymer film became soluble after 17 h and the degradation continued in solution until 73 h. The disappearance of the carbonate unit and formation of OH groups was confirmed. The obtained polyol exhibited an OH content of 2.23 mmol g^{-1}, a value that is in the range of commercially available polyols prepared from vegetable oils. This work showed the suitability of carbonate groups for the preparation of degradable polymer networks by thiol–ene reaction. The degradation products being polyols, we showed a proof of concept of their upcycling in the synthesis of polyurethane. By using simple chemistry, greener synthetic pathways and bioresources, this example opens a way for the development of more sustainable polymer networks that can reduce reliance on virgin feedstocks, minimize waste generation, and enhance overall resource efficiency.

Experimental section

Materials

All solvents were used without further purification. Water, when used in the synthesis, was deionised.

The following chemicals were used as received: chloroform-d_3 ($CDCl_3$, 99.8 atom% D, Euriso-Top), dimethyl sulfoxide-d_6 (99.8 atom% D, Euriso-Top), silica gel 60 (0.040–0.063, Sigma-Aldrich), sodium sulfate (99%, Bernd Kraft), 2,2-dimethoxy-2-phenylacetophenone (DMPA, 99%, Sigma-Aldrich), sodium chloride (99.5%, Fisher chemical), allyl alcohol (99%, Acros Organics), dimethyl carbonate (>99%, Sigma-Aldrich), 1,5,7-triazabicyclo(4.4.0)dec-5-ene (TBD, 98%, Sigma-Aldrich), vanillyl alcohol (99%, Acros Organics), palladium nanoparticles (PdNP@PVP, particles were synthesized by Dr Silke Behrens (IKFT) and analyzed by TEM, DLS and AES-ICP,[58] palladium content: 0.0404 mmol mL^{-1}), methanol (HPLC grade, VWR chemicals), tetrahydrofuran (>99.7%, VWR chemicals), thioacetic acid (96%, Sigma-Aldrich), myrcene (90%, Acros Organics), *N*,*N*-dimethylformamide (99.8%, Sigma-Aldrich), hydrochloric acid (12 M, 37%, VWR chemicals), 2-chloro-4,4,5,5-tetramethyl-1,3,2-diaxophospholane (95%, Sigma-Aldrich), chromium(III) acetylacetonate (>99% trace metals basis, Sigma-Aldrich) and *N*-hydroxy-5-norbornene-2,3-dicarboximide (97%, Sigma-Aldrich), dibutyltin dilaurate (95%, Sigma-Aldrich) and 4,4′-methylene-bis(cyclohexyl isocyanate) (90%, Fisher chemical).

Methods

Thin layer chromatography (TLC). Thin layer chromatography was carried out on silica gel coated aluminium foil (TLC silica gel F254, Sigma-Aldrich). Compounds were visualized by staining with Seebach-solution (mixture of phosphomolybdic acid hydrate, cerium(IV) sulfate, sulfuric acid and water).

Nuclear magnetic resonance (NMR). NMR spectra were recorded on BRUKER Advance DPX spectrometers (Billerica, MA) with a 5 mm dual proton/carbon probe operating at 300 MHz or 400 MHz for ^1H spectra and 75.5 MHz or 101 MHz for ^{13}C spectra, respectively. $CDCl_3$ or DMSO-d_6 were used as solvent and the resonance signals at 7.26 ppm or 2.50 ppm (^1H) and 77.16 ppm or 39.52 ppm (^{13}C) served as reference for the chemical shift δ. The spin multiplicity and corresponding signal patterns were abbreviated as follows: s = singlet, d = doublet, t = triplet, q = quartet, quint. = quintet, m = multiplet.

Gas chromatography–mass spectrometry (GC-MS). GC-MS [electron impact ionization (EI)] measurements were performed on the following system: a Varian 431 GC instrument with a capillary column FactorFour VF-5 ms (30 m × 0.25 mm × 0.25 mm) and a Varian 210 ion trap mass detector. Scans were performed from 40 to 650 m/z at rate of 1.0 scans per s. The oven temperature program was programmed as follows: initial temperature 95 °C, hold for 1 min, ramp at 15 °C min^{-1} to 220 °C, hold for 4 min, ramp at 15 °C min^{-1} to 300 °C, hold for 2 min. The injector transfer line temperature was set to 250 °C. Measurements were performed in the split–split mode (split ratio 50 : 1) using helium as carrier gas (flow rate 1.0 mL min^{-1}).

Mass spectrometry (MS). Fast atom bombardment (FAB) and Electron Ionisation (EI) mass spectra were recorded on a Finnigan MAT 95 instrument. Orbitrap Electrospray-Ionisation Mass Spectrometry (ESI-MS) mass spectra were recorded on a Q Excative (Orbitrap) mass spectrometer (Thermo Fisher Scientific, San Jose, CA, USA) equipped with an atmospheric pressure ionisation source operating in the nebuliser assisted electrospray mode. The instrument was calibrated in the m/z-range 150–2000 using a standard containing caffeine, Met-Arg-Phe-Ala acetate (MRFA) and a mixture of fluorinated phosphazenes (Ultramark 1621, all from Sigma Aldrich). A constant spray voltage of 3.5 kV, a dimensionless sheath gas of 6, and a sweep gas flow rate of 2 were applied. The capillary voltage and the S-lens RF level were set to 68.0 V and 320 °C, respectively.

Fourier-transform infrared spectroscopy (FTIR). Infrared spectra (IR) were recorded on a Bruker Alpha-p instrument in a frequency range from 3997.21 to 373.942 cm^{-1} applying ATR-technology.

UV curing. UV Curing was carried out with an Awellcure UV-LED Curing System using a lamp with 1000 mW cm^{-2} and

a wavelength of 365 nm. At the applied distance of 9 cm, an intensity of around 750 mW cm^{-2} was achieved according to spectral data provided by the manufacturer. Samples were cured at 50% power for 10 min.

Soluble part determination. Swelling properties of weighed bar samples (m_0) of the cross-linked polymers were analyzed. After immersion in THF for 24 h, the swollen samples were dried under vacuum at 100 °C overnight and weighted again (m_D) to obtain the soluble part of the networks:

$$\text{Soluble part}/\% = 100 \times (1 - m_D/m_0)$$

Differential scanning calorimetry (DSC). Differential Scanning Calorimetry (DSC) measurements were performed on DSC Q100 (TA Instruments). The polymer network was heated from −70 °C to 200 °C at a rate of 10 °C min^{-1}. Consecutive cooling and second heating run were also performed at 10 °C min^{-1}. The glass transition temperature was calculated from the second heating run. DSC analyses of the polyurethane formation are described in the experimental procedure section.

Thermogravimetric analysis (TGA). Thermogravimetric analyses (TGA) were performed on TGA-Q500 system from TA instruments at a heating rate of 10 °C min^{-1} under air.

Tensile test measurements (DMA). The tensile tests were performed on a Dynamic Mechanical Analysis instrument (DMA RSA 3 TA instrument). Tensile stress and tensile strain of the films were obtained using the DMA apparatus in traction transient mode at a rate of 10 mm min^{-1}.

A temperature sweep was performed on the same instrument. This experiment was carried out on the interval from −10 to 80 °C with a heating rate of 3 °C min^{-1} at a frequency of 1.0 Hz and a strain of 0.2%. Crosslinking density (ν_e) was calculated from classical rubbery elasticity theory: $E' = 3\nu_e RT$ with E' the storage modulus of the polymer network in the rubbery plateau region at T_α + 50 °C, R the universal constant (R = 8.314 J mol^{-1} K^{-1}), and T is the absolute temperature corresponding to E'.

Size exclusion chromatography (SEC). The degradation products were analyzed by SEC on an Ultimate 3000 system from Thermoscientific equipped with diode array detector (DAD) using dimethyformamide (DMF + lithium bromide LiBr 1 g L^{-1}) as the eluent. The system also includes a multi-angles light scattering detector (MALS) and differential refractive index detector (dRI) from Wyatt technology. Polymers were separated on two gel columns mounted in series, comprising a Shodex Asahipak GF-310 HQ column (7.5 × 300) and a Shodex Asahipak GF-510 HQ column (7.5 × 300) (exclusion limits from 500 Da to 300 000 Da). This set is preceded by a GF-1G 7B (7.5 × 50) guard column. The flow rate was kept stable at 0.5 ml min^{-1} and the column temperature was maintained at 50 °C. Easivial kit of Polystyrene from Agilent was used as the standard (M_n from 162 to 364 000 Da).

Phosphorus (^{31}P) NMR. For this analysis, the degradation product was phosphorylated using 2-chloro-4,4,5,5-tetramthyl-1,3,2-diaxophospholane (Scheme 3) and the proportions of each type of hydroxyl group was evaluated against an internal standard (*N*-hydroxy-5-norbornene-2,3-dicarboximide).[69]

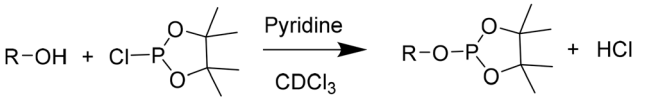

Scheme 3 Phosphorylation reaction of OH groups.

In a dry Schlenk flask, dried polyols (15.7 mg), internal standard (4.5 mg) and relaxation agent (1.5 mg) chromium(III) acetylacetonate were precisely weighted. Under an argon flow, a mixture of dry pyridine/$CDCl_3$ (0.5 mL; 1.6 : 1 vol/vol) was added. If the mixture was not homogeneous, dry DMF (0.5 mL) was added. Finally, phosphorylating reagent (0.1 mL) was added. The sample was stirred for 1 hour under argon flow. Afterwards, 0.4 mL of the mixture were transferred into an NMR tube in which 0.2 mL of dry $CDCl_3$ were added. The NMR analysis was immediately performed to prevent hydrolysis. The analysis was performed on BRUKER Advance DPX spectrometers (Billerica, MA) 400 MHz spectrometer with 512 scans, a relaxation time d1 of 5 seconds.

The chemical shifts are reported relative to the reaction product of 2-chloro-4,4,5,5-tetramethyl1,3,2-dioxaphospholane with water at 132.2 ppm. Integrals are assigned to the functional groups as followed: δ = 150.0–145.5 ppm for aliphatic hydroxyl groups, 145.5–144.7 ppm for cyclohexanol, 144.7–136.6 ppm for phenolic hydroxyl groups.

Experimental procedures

Synthesis of allyl methyl carbonate. The synthesis of allyl methyl carbonate was carried out according to literature (Scheme 4).[58]

In a round bottom flask, a mixture of allyl alcohol (1 mol, 68.3 mL) and dimethyl carbonate (631 mL, 7.5 mol, 7.50 eq.) was stirred at 80 °C for five min. Subsequently, TBD (10 mmol, 1.39 g, 0.01 eq.) was added and the reaction mixture was run for 1 hour. A mixture of dimethyl carbonate, allyl methyl carbonate and diallyl carbonate was obtained and separated by distillation. The product was distilled at 100 mbar and 70 °C yielding to allyl methyl carbonate as an oily compound.

Yield: 28%.

^{1}H-NMR (400 MHz, $CDCl_3$) δ/ppm = 5.96–5.87 (m, 1H), 5.37–5.23 (m, 2H), 4.62–4.60 (m, 2H), 3.77 (s, 3H).

^{13}C-NMR (101 MHz, $CDCl_3$) δ/ppm = 155.70, 131.70, 118.91, 68.56, 54.88.

IR (ATR platinum diamond): ν/cm^{-1} = 2959.3, 1745.5, 1650.6, 1444.1, 1365.1, 1249.1, 965.0, 927.5, 790.8, 555.2.

Synthesis of allylated vanillyl alcohol AVA ((4-(allyloxy)-3-methoxyphenyl)methanol). The synthesis of allylated vanillyl alcohol **AVA** was carried out according to literature.[58]

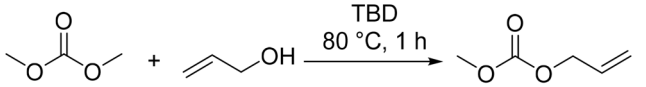

Scheme 4 Synthesis of allyl methyl carbonate from DMC and allyl alcohol.

In a round bottom flask, vanillyl alcohol (64.9 mmol, 10 g) was mixed with allyl methyl carbonate (162 mmol, 18.8 g, 2.5 eq.) and triphenylphosphine (3.25 mmol, 851 mg, 0.05 eq.) in water (90 mL). Palladium nanoparticles stabilized in water (PdNP@PVP, 0.10 mol%, 64.9 μmol, 1.60 mL) were added to the mixture and the reaction was stirred at 90 °C for 16 hours. The reaction mixture was poured in a separation funnel and extracted with ethyl acetate. The combined organic phases were dried over sodium sulfate and solvent was removed under reduced pressure. The crude mixture was purified by column chromatography (eluent cyclohexane/EtOAc; 7/3, vol/vol) to give **AVA**.

Yield: 75%.

R_f = 0.45 (cyclohexane/EtOAc; 5/5, vol/vol).

^{1}H-NMR (300 MHz, DMSO-d_6) δ/ppm = 6.93–6.63 (m, 3H), 6.09–5.96 (m, 1H), 5.40–5.21 (m, 2H), 5.07 (t, J = 5.7 Hz, 1H), 4.51 (d, J = 3.9 Hz, 2H), 4.41 (d, J = 5.5 Hz, 2H), 3.75 (s, 3H).

^{13}C-NMR (75 MHz, DMSO-d_6) δ/ppm = 148.93, 146.38, 135.51, 134.06, 118.49, 117.33, 113.44, 110.80, 69.09, 62.78, 55.42.

IR (ATR platinum diamond): ν/cm^{-1} = 3330.9, 2993.4, 2906.2, 2856.2, 2354.3, 2157.7, 2033.5, 1860.9, 1646.6, 1591.6, 1512.7, 1454.9, 1417.9, 1365.1, 1319.3, 1294.0, 1252.2, 1232.6, 1136.9, 1059.6, 1022.8, 1005.0, 989.0, 925.7, 916.5, 853.5, 820.2, 802.6, 739.7, 642.2, 606.0, 592.4, 575.2, 522.1, 462.538, 409.7.

EI-HRMS of $C_{11}H_{14}O_3$ $[M]^+$ calculated: 194.0937, found: 194.0937.

Synthesis of AVACarb (bis(4-(allyloxy)-3-methoxybenzyl) carbonate). In a round bottomed-flask, **AVA** compound (5.15 mmol, 1 g) was dissolved in dimethyl carbonate (51.5 mmol, 4.64 g, 10.0 eq.). To this solution, TBD (258 μmol, 5.00 mol%, 35.8 mg) was added and the mixture was heated to 80 °C under reflux for 6 hours during which the progress of the reaction was checked *via* TLC. Unreacted dimethyl carbonate was removed with the rotary evaporator. Then, additional **AVA** compound (5.41 mmol, 1.05 g, 1.05 eq.) was added and the mixture was heated to 100 °C under reflux for 24 hours. After completion of the reaction, as monitored using TLC, ethyl acetate (30 mL) was added to the reaction mixture. The organic phase was washed three times with water (30 mL) and with brine (30 mL), dried over sodium sulfate and solvents were removed under vacuum. The crude product was purified *via* column chromatography (eluent cyclohexane/EtOAc, from 95 : 5 to 7 : 3, vol/vol) to obtain **AVAcarb** as a white solid.

Yield: 67%.

R_f: 0.56 (cyclohexane/EtOAc; 6/4, vol/vol).

^{1}H-NMR (400 MHz, DMSO-d_6) δ/ppm: 7.00–6.89 (m, 6H), 6.07–5.98 (m, 2H), 5.40–5.22 (m, 4H, H10), 5.06 (s, 4H), 4.54 (dt, J = 5.3, 1.4 Hz, 4H), 3.74 (s, 6H).

^{13}C-NMR (101 MHz, DMSO-d_6) δ/ppm: 154.46, 148.91, 147.77, 133.75, 128.00, 121.15, 117.55, 113.18, 112.60, 69.10, 68.90, 55.50.

IR (ATR platinum diamond): ν/cm^{-1}: 2963.1, 2835.8, 1742.3, 1649.6, 1604.8, 1590.6, 1513.4, 1453.5, 1421.5, 1376.3, 1328.9, 1253.0, 1223.6, 1195.1, 1165.2, 1134.0, 1021.5, 917.4, 905.1, 886.3, 852.6, 801.3, 787.2, 738.2, 663.0, 633.3, 617.0, 550.7, 518.8, 468.1, 420.2.

FAB-HRMS of $C_{23}H_{26}O_7$ $[M]^+$ calculated: 414.1673, found: 414.1674.

Synthesis of myrcene trithiol (3-(mercaptomethyl)-7-methyloctane-1,6-dithiol). The synthesis of myrcene-based trithiol was carried out according to literature.[60]

In a round bottom flask, myrcene compound (36.7 mmol, 5 g) was mixed with thioacetic acid (132 mmol, 9.44 mL, 3.6 eq.) under ice cooling. The mixture was stirred at room temperature for 23 hours. The thioacetic acid was partly removed under reduced pressure. Subsequently, TBD (5.51 mmol, 766 mg, 0.15 eq.) and MeOH (45 mL, 1.1 mol, 30 eq.) were added and the solution was stirred at 75 °C for 25 hours. The solvent was removed under reduced pressure and the product was isolated by column chromatography (eluent from 0.5% to 1% of EtOAc in cyclohexane, vol/vol). The desired product was obtained as a mixture of isomers. Because of the indistinct NMR spectra (Fig. S4†), the product was identified *via* mass spectrometry and elemental analysis.

Yield: 59%.

R_f = 0.61 (cyclohexane/EtOAc; 98 : 2, vol/vol).

IR (ATR platinum diamond): ν (cm^{-1}): 2958.7, 2924.9, 2867.9, 2548.7, 1452.2, 1382.7, 1366.3, 1329.2, 1247.7, 1080.0, 921.6, 873.1, 809.4, 765.9, 713.5, 660.8, 468.9.

EI-HRMS of $C_{10}H_{22}S_3$ $[M]^+$ calculated: 238.0878, found: 238.0882.

Elemental analysis: calculated: C 50.37%, H 9.30%, S 40.33; found: C 50.67%, H 8.61%, S 38.67%.

Thiol–ene polymerization. AVACarb (0.13 mmol, 55.2 mg) was mixed with myrcene trithiol (0.09 mmol, 21.2 mg) in a double bond : thiol ratio of 1 : 1. Then, DMPA (5 mol% per double bond, 3.30 mg) was added. After thorough mixing, the mixture was transferred to a glass plate with tape boundaries (1 cm × 2.5 cm). Solid samples were gently melted using a heatgun to ensure homogeneous film formation. The hot samples were placed into the UV oven and the curing was carried out under UV irradiation (365 nm, 50% power) for 10 min.

IR (ATR platinum diamond): ν/cm^{-1} = 2931.7, 1738.9, 1592.2, 1513.3, 1462.6, 1421.1, 1386.2, 1366.0, 1334.6, 1224.3, 1162.1, 1138.0, 1026.5, 908.7, 852.0, 789.5, 650.0, 552.3, 461.2.

Degradation of AVACarb. AVACarb (26 mg) was immersed in the solvent mixture (2 mL) and heated up to the desire temperature. The conversion of **AVACarb** into **AVA** was monitored by SEC. 92% of the **AVACarb** was degraded into **AVA** in 46 h in DMF/HCl 1 M at 100 °C.

Degradation of the polymer network. The polymer network (160 mg) was immersed in a mixture of DMF (5.7 mL) and HCl (0.48 mL) in a Schlenk flask. The flask was heated at 100 °C. Once the polymer network became soluble, the reaction medium was directly analyzed by SEC. After 120 h, the product was dried under vacuum before ^{31}P NMR analysis.

Repolymerization into polyurethane. In a DSC pan, polyols (2.03 mmol g^{-1} of OH content, 5 mg) were mixed with 4,4′-methylene-bis(cyclohexyl isocyanate) (HMDI, 5.6 mmol, 1.4 μL)

and a catalytic amount of dibutyltin dilaurate. The DSC pan was hermetically closed with a lid and the sample was heated from 0 °C to 150 °C (Fig. S15†) before being cooled down to −20 °C, both at a rate of 10 °C min^{-1} (Fig. S16†). Of note, the experiment was replicated in which the DSC pan was put in the oven at 50 °C for 1 hour and at 100 °C for 2 hours. Similar FTIR spectrum and DSC thermogram were obtained.

Conflicts of interest

There are no conflicts to declare.

Acknowledgements

Dr A. Llevot acknowledges the Ministry of Science, Research and Arts of Baden-Wuerttemberg, MWK, for the Research Seed Capital (RiSC) funding. The authors would like to thank Emmanuel Ibarboure, Frédérique Ham Pichavant and Maëva Peloille for their respective help with the tensile test measurements, mass spectrometry and ^{13}P NMR.

References

1 J. Liu, L. Zhang, W. Shun, J. Dai, Y. Peng and X. Liu, *J. Polym. Sci.*, 2021, **59**, 1474–1490.
2 R. L. Quirino, K. Monroe, C. H. Fleischer III, E. Biswas and M. R. Kessler, *Polym. Int.*, 2021, **70**, 167–180.
3 E. Feghali, K. M. Torr, D. J. van de Pas, P. Ortiz, K. Vanbroekhoven, W. Eevers and R. Vendamme, *Top. Curr. Chem.*, 2018, **376**, 32.
4 A. Llevot, *J. Am. Oil Chem. Soc.*, 2017, **94**, 169–186.
5 F. H. Isikgor and C. R. Becer, *Polym. Chem.*, 2015, **6**, 4497–4559.
6 D. J. Fortman, J. P. Brutman, G. X. De Hoe, R. L. Snyder, W. R. Dichtel and M. A. Hillmyer, *ACS Sustainable Chem. Eng.*, 2018, **6**, 11145–11159.
7 H. Sun, C. P. Kabb, Y. Dai, M. R. Hill, I. Ghiviriga, A. P. Bapat and B. S. Sumerlin, *Nat. Chem.*, 2017, **9**, 817–823.
8 C. J. Kloxin and C. N. Bowman, *Chem. Soc. Rev.*, 2013, **42**, 7161–7173.
9 M. Chen, Y. Gu, A. Singh, M. Zhong, A. M. Jordan, S. Biswas, L. T. J. Korley, A. C. Balazs and J. A. Johnson, *ACS Cent. Sci.*, 2017, **3**, 124–134.
10 A. Beziau, A. Fortney, L. Fu, C. Nishiura, H. Wang, J. Cuthbert, E. Gottlieb, A. C. Balazs, T. Kowalewski and K. Matyjaszewski, *Polymer*, 2017, **126**, 224–230.
11 Y. Jin, Z. Lei, P. Taynton, S. Huang and W. Zhang, *Matter*, 2019, **1**, 1456–1493.
12 D. Montarnal, M. Capelot, F. Tournilhac and L. Leibler, *Science*, 2011, **334**, 965–968.
13 T. Vidil and A. Llevot, *Macromol. Chem. Phys.*, 2022, **223**, 2100494.
14 J. Liu, S. Wang, Y. Peng, J. Zhu, W. Zhao and X. Liu, *Prog. Polym. Sci.*, 2021, **113**, 101353.
15 X.-L. Zhao, P.-X. Tian, Y.-D. Li and J.-B. Zeng, *Green Chem.*, 2022, **24**, 4363–4387.
16 A. Liguori and M. Hakkarainen, *Macromol. Rapid Commun.*, 2022, **43**, 2100816.
17 X.-L. Zhao, Y.-D. Li and J.-B. Zeng, *Polym. Chem.*, 2022, **13**, 6573–6588.
18 A. Kumar and L. A. Connal, *Macromol. Rapid Commun.*, 2023, **44**, 2200892.
19 M. A. Lucherelli, A. Duval and L. Avérous, *Prog. Polym. Sci.*, 2022, **127**, 101515.
20 J. Wan, J. Zhao, X. Zhang, H. Fan, J. Zhang, D. Hu, P. Jin and D.-Y. Wang, *Prog. Polym. Sci.*, 2020, **108**, 101287.
21 M. Fache, B. Boutevin and S. Caillol, *Eur. Polym. J.*, 2015, **68**, 488–502.
22 A. Llevot, E. Grau, S. Carlotti, S. Grelier and H. Cramail, *Macromol. Rapid Commun.*, 2016, **37**, 9–28.
23 F. Ng, G. Couture, C. Philippe, B. Boutevin and S. Caillol, *Molecules*, 2017, **22**, 149.
24 E. A. Baroncini, S. Kumar Yadav, G. R. Palmese and J. F. Stanzione III, *J. Appl. Polym. Sci.*, 2016, **133**, 44103.
25 Z. Zhou, X. Su, J. Liu and R. Liu, *ACS Appl. Polym. Mater.*, 2020, **2**, 5716–5725.
26 Y. Xu, K. Odelius and M. Hakkarainen, *ACS Sustainable Chem. Eng.*, 2020, **8**, 17272–17279.
27 V.-D. Mai, S.-R. Shin, D.-S. Lee and I. Kang, *Polymers*, 2019, **11**, 293.
28 S. Wang, S. Ma, Q. Li, X. Xu, B. Wang, W. Yuan, S. Zhou, S. You and J. Zhu, *Green Chem.*, 2019, **21**, 1484–1497.
29 Q. Yu, X. Peng, Y. Wang, H. Geng, A. Xu, X. Zhang, W. Xu and D. Ye, *Eur. Polym. J.*, 2019, **117**, 55–63.
30 S. Wang, S. Ma, Q. Li, W. Yuan, B. Wang and J. Zhu, *Macromolecules*, 2018, **51**, 8001–8012.
31 H. Geng, Y. Wang, Q. Yu, S. Gu, Y. Zhou, W. Xu, X. Zhang and D. Ye, *ACS Sustainable Chem. Eng.*, 2018, **6**, 15463–15470.
32 M. A. Rashid, M. N. Hasan, M. A. R. Dayan, M. S. Ibna Jamal and M. K. Patoary, *Reactions*, 2023, **4**, 66–91.
33 L. Jiang, Y. Tian, J. Cheng and J. Zhang, *Polym. Chem.*, 2021, **12**, 6527–6537.
34 K. Hong, Q. Sun, X. Zhang, L. Fan, T. Wu, J. Du and Y. Zhu, *ACS Sustainable Chem. Eng.*, 2022, **10**, 1036–1046.
35 L. Jiang, Y. Tian, X. Wang, J. Zhang, J. Cheng and F. Gao, *Polym. Chem.*, 2023, **14**, 862–871.
36 L. Xiaohong, L. Liyan, L. Maoping, S. Xuan, L. Hehua and C. Guoyang, *Polymer*, 2020, **210**, 123030.
37 H. Memon, Y. Wei and C. Zhu, *Mater. Today Commun.*, 2021, **29**, 102814.
38 A. Roig, P. Hidalgo, X. Ramis, S. De la Flor and À. Serra, *ACS Appl. Polym. Mater.*, 2022, **4**, 9341–9350.
39 M. A. Rashid, M. M. Mian, Y. Wei and W. Liu, *Mater. Today Commun.*, 2023, **35**, 106178.
40 Y. Sun, D. Sheng, H. Wu, X. Tian, H. Xie, B. Shi, X. Liu and Y. Yang, *Polymer*, 2021, **233**, 124208.

41 D.-M. Xie, D.-X. Lu, X.-L. Zhao, Y.-D. Li and J.-B. Zeng, *Ind. Crops Prod.*, 2021, **174**, 114198.
42 H. Wang, Y. Fu, Y. Liu, J. Li, X. Sun and T. Liu, *Eur. Polym. J.*, 2023, **196**, 112309.
43 S. Grauzeliene, M. Kastanauskas, V. Talacka and J. Ostrauskaite, *ACS Appl. Polym. Mater.*, 2022, **4**, 6103–6110.
44 X. Xu, S. Ma, S. Wang, J. Wu, Q. Li, N. Lu, Y. Liu, J. Yang, J. Feng and J. Zhu, *J. Mater. Chem. A*, 2020, **8**, 11261–11274.
45 S. Engelen, A. A. Wróblewska, K. De Bruycker, R. Aksakal, V. Ladmiral, S. Caillol and F. E. Du Prez, *Polym. Chem.*, 2022, **13**, 2665–2673.
46 S. Guggari, F. Magliozzi, S. Malburet, A. Graillot, M. Destarac and M. Guerre, *ACS Sustainable Chem. Eng.*, 2023, **11**, 6021–6031.
47 S. Ma and D. C. Webster, *Prog. Polym. Sci.*, 2018, **76**, 65–110.
48 S. L. Buchwalter and L. L. Kosbar, *J. Polym. Sci., Part A: Polym. Chem.*, 1996, **34**, 249–260.
49 M. Shen, R. Almallahi, Z. Rizvi, E. Gonzalez-Martinez, G. Yang and M. L. Robertson, *Polym. Chem.*, 2019, **10**, 3217–3229.
50 M. Shen and M. L. Robertson, *ACS Sustainable Chem. Eng.*, 2021, **9**, 438–447.
51 Z. Gao, Y. You, Q. Chen, M. North and H. Xie, *Green Chem.*, 2023, **25**, 172–182.
52 S. Wenjie, Z. Lei, X. Jiazhu, C. Binlong and C. Yonghong, *Mater. Lett.*, 2022, **323**, 132589.
53 M. Jinpeng, L. Guanxi, H. Xueni, L. Ning, L. Zhe, Z. Fan, Y. Liangliang, C. Xue, S. Lei and A. Yuhui, *Polym. Degrad. Stab.*, 2022, **201**, 109989.
54 M. Ge, J.-T. Miao, K. Zhang, Y. Wu, L. Zheng and L. Wu, *Polym. Chem.*, 2021, **12**, 564–571.
55 W. Zhang, F. Gao, X. Chen, L. Shen, Y. Chen and Y. Lin, *ACS Sustainable Chem. Eng.*, 2023, **11**, 3065–3073.
56 L. Wang, H. Li and C. P. Wong, *J. Polym. Sci., Part A: Polym. Chem.*, 2000, **38**, 3771–3782.
57 R. L. Snyder, D. J. Fortman, G. X. De Hoe, M. A. Hillmyer and W. R. Dichtel, *Macromolecules*, 2018, **51**, 389–397.
58 A. Llevot, B. Monney, A. Sehlinger, S. Behrens and M. A. R. Meier, *Chem. Commun.*, 2017, **53**, 5175–5178.
59 H. Mutlu, J. Ruiz, S. C. Solleder and M. A. R. Meier, *Green Chem.*, 2012, **14**, 1728–1735.
60 M. Firdaus, M. A. R. Meier, U. Biermann and J. O. Metzger, *Eur. J. Lipid Sci. Technol.*, 2014, **116**, 31–36.
61 P. Saint-louis-Augustin, G. Fremy, B. Monguillon and L. Corbel, *US Pat.,* US20200010412A1, 2020.
62 G. Yang, S. L. Kristufek, L. A. Link, K. L. Wooley and M. L. Robertson, *Macromolecules*, 2016, **49**, 7737–7748.
63 J. Xue, X. Yang, Y. Ke, Z. Yan, X. Dong, Y. Luo and C. Zhang, *Ind. Crops Prod.*, 2021, **171**, 113956.
64 L. Pezzana, G. Melilli, P. Delliere, D. Moraru, N. Guigo, N. Sbirrazzuoli and M. Sangermano, *Prog. Org. Coat.*, 2022, **173**, 107203.
65 J. Bernard, E.-M. Köck, R. G. Huber, K. R. Liedl, L. Call, R. Schlögl, H. Grothe and T. Loerting, *RSC Adv.*, 2017, **7**, 22222–22233.
66 A. Dibenedetto, M. Aresta, P. Giannoccaro, C. Pastore, I. Pápai and G. Schubert, *Eur. J. Inorg. Chem.*, 2006, **2006**, 908–913.
67 C. M. Comisar, S. E. Hunter, A. Walton and P. E. Savage, *Ind. Eng. Chem. Res.*, 2008, **47**, 577–584.
68 J. Østergaard and C. Larsen, *Molecules*, 2007, **12**, 2396–2412.
69 A. Granata and D. S. Argyropoulos, *J. Agric. Food Chem.*, 1995, **43**, 1538–1544.
70 H. Sardon, D. Mecerreyes, A. Basterretxea, L. Avérous and C. Jehanno, *ACS Sustainable Chem. Eng.*, 2021, **9**, 10664–10677.

